Probing Individual Environmental Bacteria for Viruses by Using Microfluidic Digital PCR

Arbel D. Tadmor, *et al.*

Science **333**, 58 (2011);
DOI: 10.1126/science.1200758

suggest that there are unknown aspects of transcription and/or posttranscriptional processing of RNA. These differences may now be studied along with those in other genomes and organisms such as the mitochondrial genomes of trypanosomes and chloroplasts of plants, where RNA editing and modifications are relatively common (*36*, *37*).

The underlying mechanisms for these events are largely unknown. For most of the cases, we do not know yet whether a different base was incorporated into the RNA during transcription or if these events occur posttranscriptionally. About 23% of the sites are A-to-G differences; some of these are likely mediated by ADAR, but other, currently unknown, mechanisms can be involved. If it is a cotranscriptional process, then the signal can be in the DNA or the RNA such as secondary structures or modified nucleotides. In addition, as some of the RDDs are found near splice and poly(A) sites, it is possible that this may be a facet of systematic RNA processing steps such as splicing and cleavage (*38*, *39*).

Our findings supplement previous studies demonstrating RNA-DNA differences in the human genome and show that these differences go beyond A-to-G transition. These findings affect our understanding of genetic variation; in addition to DNA sequence variation, we identify individual variation in RNA sequences. For monomorphic DNA sequences that show RDD, there is an overall increase in genetic variation. Thus, this variation not only contributes to individual variation in gene expression, but also diversifies the proteome because some identified sites lead to nonsynonymous amino acid changes. We speculate that this RNA sequence variation likely affects disease susceptibility and manifestations. To date, mapping studies have focused on identifying DNA variants as disease susceptibility alleles. Our results suggest that the search may need to include RNA sequence variants that are not in the DNA sequences.

References and Notes

1. R. T. Libby, J. A. Gallant, *Mol. Microbiol.* **5**, 999 (1991).
2. J. F. Sydow, P. Cramer, *Curr. Opin. Struct. Biol.* **19**, 732 (2009).
3. S. H. Chen *et al.*, *Science* **238**, 363 (1987).
4. L. M. Powell *et al.*, *Cell* **50**, 831 (1987).
5. B. L. Bass, H. Weintraub, *Cell* **55**, 1089 (1988).
6. J. B. Li *et al.*, *Science* **324**, 1210 (2009).
7. A. Athanasiadis, A. Rich, S. Maas, *PLoS Biol.* **2**, e391 (2004).
8. M. J. Thomas, A. A. Platas, D. K. Hawley, *Cell* **93**, 627 (1998).
9. D. Wang *et al.*, *Science* **324**, 1203 (2009).
10. N. Zenkin, Y. Yuzenkova, K. Severinov, *Science* **313**, 518 (2006).
11. M. Sakurai, T. Yano, H. Kawabata, H. Ueda, T. Suzuki, *Nat. Chem. Biol.* **6**, 733 (2010).
12. K. Nishikura, *Annu. Rev. Biochem.* **79**, 321 (2010).
13. E. Y. Levanon *et al.*, *Nat. Biotechnol.* **22**, 1001 (2004).
14. S. G. Conticello, *Genome Biol.* **9**, 229 (2008).
15. A. Chester, J. Scott, S. Anant, N. Navaratnam, *Biochim. Biophys. Acta-Gene Struct. Expression* **1494**, 1 (2000).
16. J. Dausset *et al.*, *Genomics* **6**, 575 (1990).
17. International HapMap Consortium, *Nature* **426**, 789 (2003).
18. International HapMap Consortium, *Nature* **437**, 1299 (2005).
19. The 1000 Genomes Project Consortium, *Nature* **467**, 1061 (2010).
20. H. M. Cann, *Curr. Opin. Genet. Dev.* **2**, 393 (1992).
21. T. C. Matise *et al.*, *Am. J. Hum. Genet.* **73**, 271 (2003).
22. F. Sanger, S. Nicklen, A. R. Coulson, *Proc. Natl. Acad. Sci. U.S.A.* **74**, 5463 (1977).
23. D. R. Bentley *et al.*, *Nature* **456**, 53 (2008).
24. J. Harrow *et al.*, *Genome Biol.* **7** (suppl. 1), S4 (2006).
25. Supporting material is available on *Science* Online.
26. S. B. Montgomery *et al.*, *Nature* **464**, 773 (2010).
27. C. Trapnell *et al.*, *Nat. Biotechnol.* **28**, 511 (2010).
28. B. R. Rosenberg, C. E. Hamilton, M. M. Mwangi, S. Dewell, F. N. Papavasiliou, *Nat. Struct. Mol. Biol.* **18**, 230 (2011).
29. S. F. Altschul, W. Gish, W. Miller, E. W. Myers, D. J. Lipman, *J. Mol. Biol.* **215**, 403 (1990).
30. K. L. Sodek *et al.*, *Mol. Biosyst.* **4**, 762 (2008).
31. A. Michalski, J. Cox, M. Mann, *J. Proteome Res.* **10**, 1785 (2011).
32. L. M. de Godoy *et al.*, *Genome Biol.* **7**, R50 (2006).
33. C. M. Burns *et al.*, *Nature* **387**, 303 (1997).
34. H. Lomeli *et al.*, *Science* **266**, 1709 (1994).
35. S. Maas, S. Patt, M. Schrey, A. Rich, *Proc. Natl. Acad. Sci. U.S.A.* **98**, 14687 (2001).
36. C. G. Phreaner, M. A. Williams, R. M. Mulligan, *Plant Cell* **8**, 107 (1996).
37. H. A. Hundley, A. A. Krauchuk, B. L. Bass, *RNA* **14**, 2050 (2008).
38. S. M. Rueter, C. M. Burns, S. A. Coode, P. Mookherjee, R. B. Emeson, *Science* **267**, 1491 (1995).
39. S. M. Rueter, T. R. Dawson, R. B. Emeson, *Nature* **399**, 75 (1999).

Acknowledgments: Dedicated to the memory of Dr. Tom Kadesch who gave us important suggestions, taught us salient and subtle points on gene expression, and inspired us with his enthusiasm. Dr. Kadesch died during the preparation of this manuscript. We thank D. Epstein, H. Kazazian, D. Puppione, and L. Simpson for suggestions and discussions. We thank C. Gunter, R. Nussbaum, and J. Puck for comments on the manuscript, M. Morley for help with data analysis, W. Ankener for sample processing, and J. Devlin and CHOP NAP core for results on Sanger sequencing. The mass spectrometry analysis was carried out at the Wistar Proteomic Facility; we thank K. Speicher for help and suggestions. Funded by grants from the National Institutes of Health (to V.G.C. and M.L.) and support from the Howard Hughes Medical Institute. The RNA-Seq data have been deposited in the National Center for Biotechnology Information's Gene Expression Omnibus under the accession no. GSE25840.

Supporting Online Material

www.sciencemag.org/cgi/content/full/science.1207018/DC1
Materials and Methods
Figs. S1 to S5
Tables S1 to S10
References (*40*–*44*)

3 March 2011; accepted 10 May 2011
Published online 19 May 2011;
10.1126/science.1207018

Probing Individual Environmental Bacteria for Viruses by Using Microfluidic Digital PCR

Arbel D. Tadmor,[1]* Elizabeth A. Ottesen,[2] Jared R. Leadbetter,[3] Rob Phillips[4]*

Viruses may very well be the most abundant biological entities on the planet. Yet neither metagenomic studies nor classical phage isolation techniques have shed much light on the identity of the hosts of most viruses. We used a microfluidic digital polymerase chain reaction (PCR) approach to physically link single bacterial cells harvested from a natural environment with a viral marker gene. When we implemented this technique on the microbial community residing in the termite hindgut, we found genus-wide infection patterns displaying remarkable intragenus selectivity. Viral marker allelic diversity revealed restricted mixing of alleles between hosts, indicating limited lateral gene transfer of these alleles despite host proximity. Our approach does not require culturing hosts or viruses and provides a method for examining virus-bacterium interactions in many environments.

Despite the pervasiveness of bacteriophages in nature and their postulated impact on diverse ecosystems (*1*), we have a poor grasp of the biology of these viruses and their host specificity in the wild. Although substantial progress has been made with certain host-virus systems such as cyanophages (*2*–*5*), this is the exception rather than the rule. Conventional plaque assays used to isolate environmental viruses are not applicable to >99% of microbes in nature because the vast preponderance of the microbial diversity on Earth has yet to be cultured in vitro (*6*). Given the magnitude of the problem, the development of high-throughput, massively parallel sequencing approaches that do not rely on cultivation to identify specific virus-host relations are required. Although metagenomics has revolutionized our understanding of viral diversity on Earth (*7*–*9*), that approach

[1]Department of Biochemistry and Molecular Biophysics, California Institute of Technology, Pasadena, CA 91125, USA. [2]Department of Civil and Environmental Engineering, Massachusetts Institute of Technology, Cambridge, MA 02139, USA. [3]Ronald and Maxine Linde Center for Global Environmental Science, California Institute of Technology, Pasadena, CA 91125, USA. [4]Departments of Applied Physics and Bioengineering, California Institute of Technology, Pasadena, CA 91125, USA.

*To whom correspondence should be addressed. E-mail: arbel@caltech.edu (A.D.T.); phillips@pboc.caltech.edu (R.P.)

has as yet done little to shed light on the nature of specific viral-host interactions, except in restricted cases (*10*).

Recent advances in microfluidic technology have enabled the isolation and analysis of single cells from nature (*11*–*13*). We present an alternative to the classical phage enrichment technique where we use an uncultured virus to capture its hosts from the environment with a microfluidic polymerase chain reaction (PCR) approach called digital multiplex PCR (*12*, *14*). To this end, microbial cells were harvested directly from the environment, diluted, and loaded onto a digital PCR array panel containing 765 PCR chambers operating at single-molecule sensitivity. Samples were diluted such that the majority of chambers were ideally either empty or contained a single bacterium (Fig. 1), achieving a Poisson distribution (*15*). Because there is no universally conserved gene in viruses (*7*, *16*), we designed degenerate primers (*17*) to target a subgroup of diverse phagelike elements (*18*). Concurrently, the small subunit ribosomal RNA (SSU rRNA) gene encoded by each bacterial cell was amplified by using universal "all bacterial" primers (see fig. S1 for experimental design). Possible genuine host-virus associations detectable by this assay are depicted in Fig. 1C. Free phages may also colocalize with hosts; however, these events are not expected to lead to statistically significant colocalizations because of the random nature of these associations (*19*).

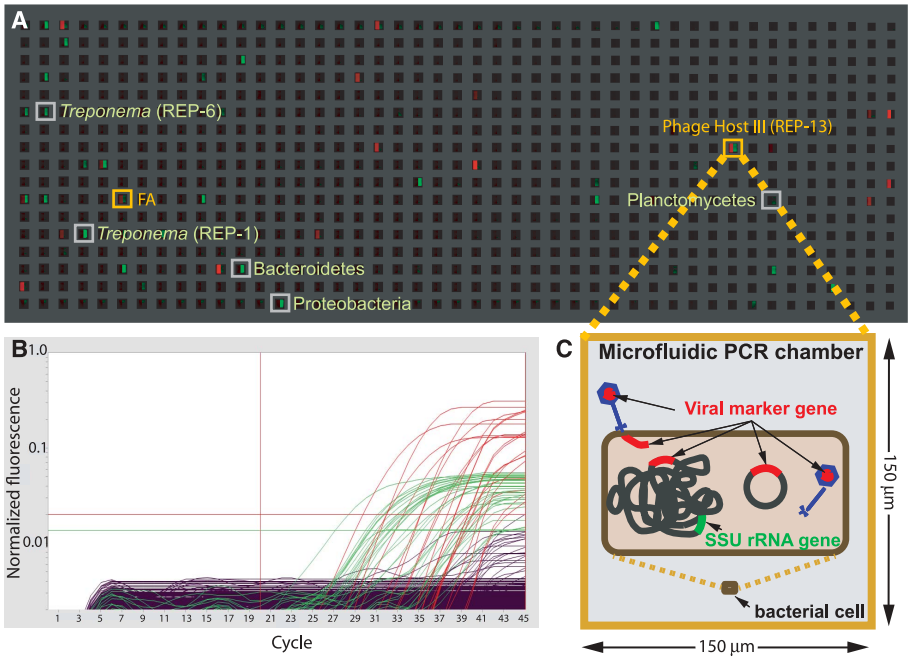

Fig. 1. End-point fluorescence measured in a panel of a microfluidic digital PCR array. (**A**) The measured end-point fluorescence from the rRNA channel (right half of each chamber, with the left half masked) and the terminase channel (left half of each chamber, with the right half masked) in a microfluidic array panel. Each panel in the array (1 of 12) consists of 765 reaction chambers 150 μm by 150 μm by 270 μm (6 nl). Retrieved colocalizations are outlined in orange, and positive rRNA chambers randomly selected for retrieval are outlined in gray. FA indicates false alarm (a probable terminase primer-dimer). (**B**) Normalized amplification curves of all chambers in (A) after linear derivative baseline correction (red, viral; green, rRNA). (**C**) Specific physical associations between a bacterial cell and the viral marker gene resulting in colocalization include, for example, an attached or assembling virion, injected DNA, an integrated prophage, or a plasmid containing the viral marker gene.

Hunting for phages in the termite hindgut. The system we chose to investigate was the termite hindgut. This microliter-in-scale environment contains ~10^7 prokaryotic cells per μl (*20*) with over 250 different species of bacteria (*21*), making it ideally suited to explore many potential, diverse phage-host interactions. To find a viral marker gene relevant to such an environment, we examined the more abundant candidate viral marker genes present in the sequenced metagenome from a hindgut of a higher termite from Costa Rica collected in 2005 (*22*) [table S1;

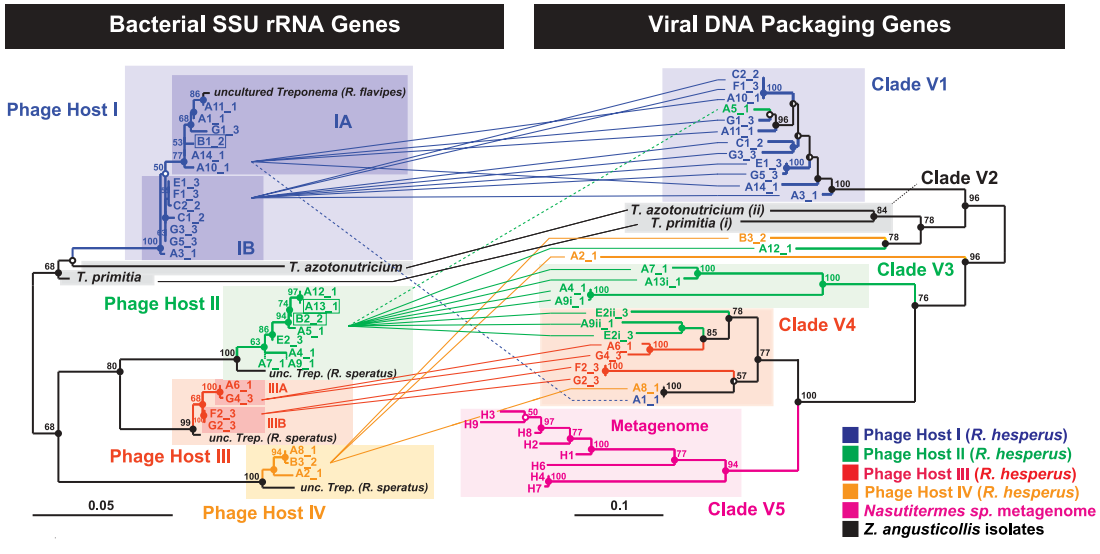

Fig. 2. Phylogenetic relationship between cultured and uncultured bacterial host rRNA genes and their associated viral DNA packaging genes. (**Left**) Maximum likelihood (ML) tree of 898 unambiguous nucleotides of the SSU rRNA gene of ribotypes that repeatedly colocalized with the terminase gene, including the two isolated spirochetes *Treponema primitia* and *Treponema azotonutricium*. Shorter sequences (A7, 780 bp, and A9, 806 bp) were added by parsimony (dashed branches). (**Right**) ML tree of 705 unambiguous nucleotides of the large terminase subunit gene. Connecting lines represent colocalized pairs, revealing restricted mixing of terminase alleles between different bacterial hosts. For association of three additional recombinant sequences (boxed on the left), see fig. S5. Statistically, we estimate that an average of 0.6 colocalizations are false [~2% error (*19*)]. The sequence error rates (*40*) for the rRNA and terminase genes were measured to be 0 (n = 8) and <0.6 ± 0.3% SD (n = 9), respectively (*18*). Alleles are named by array (A to G) and retrieval index followed by an underscore and the colony number (colony 1 being sampled 6 months before colonies 2 and 3). Lowercase roman numerals indicate multiple terminases per chromosome. Scale bars represent substitutions per alignment. For interpretation of node support, refer to (*18*), and for accession numbers, table S10.

search algorithm described in (*18*)]. We then checked whether any of these viral genes had homologous counterparts in the sequenced genomes of two spirochetes isolated in 1997 from a laboratory colony of genetically and geographically distant termites originally collected in 1986 from Northern California (*23*, *24*). We identified two such genes encoding a large terminase subunit protein (homologous to the T4-associated pfam03237 Terminase_6) and a portal protein (homologous to pfam04860 Phage_portal) exhibiting about 70 to 78% amino acid identity to their closest homologs in the higher termite gut metagenome (table S2). This finding is unexpected given that typically, across biology, portal proteins and terminase proteins from different phages exhibit little overall sequence similarity (*25*–*28*). Further analysis revealed that the spirochete viral genes were part of a larger prophage-like element, with the majority of recognizable genes most closely related to *Siphoviridae* phage genes (*19*). The association of these genes with prophage-like elements is consistent with the fact that both the Terminase_6 pfam and the Phage_portal pfam describe proteins in known lysogenic and lytic phages.

As a viral marker gene for this prophage-like element, we chose the large terminase subunit gene. This gene is a component of the DNA packaging and cleaving mechanism present in numerous double-stranded DNA phages (*26*) and is considered to be a signature of phages (*29*). We consequently designed degenerate primers on the basis of the collection of 50 metagenome and treponeme-isolate alleles of this gene. The ~820–base pair (bp) amplicon spanned by these primers covered about two-thirds of this gene and about 77% of the predicted N-terminal domain containing the conserved adenosine triphosphatase (ATPase) center (*26*, *30*), the "engine" of this DNA packaging motor (*31*) (see alignments in figs. S2 and S3). Testing these primers against the RefSeq viral database (*32*) did not yield any hits (fig. S2). Indeed, the closest homolog of this gene in the RefSeq viral database displayed only 25% amino acid identity (table S2). Thus, although this terminase gene was associated with the Terminase_6 pfam, the termite-related alleles appear to be part of a novel assemblage of terminase genes in this environment and not closely related to previously sequenced phages (fig. S2).

Given that terminase genes of different phages often exhibit less sequence similarity (see above), the fact that we found such closely related terminase genes from such distantly related termites collected from well-separated geographical locations (California and Costa Rica) and from specimens collected almost two decades apart led us to speculate that this family of viral genes and prophage-like elements might be ubiquitous in termites. Indeed, to date we have identified close homologs of the large terminase subunit gene in the gut communities of nine termite species belonging to four families collected from five different geographical locations. We therefore wished to identify the bacterial hosts associated with this viral marker gene. To this end, we collected representatives of a third previously unexamined termite family (Rhinotermitidae; *Reticulitermes hesperus*, from a third geographical location in Southern California) over a span of 6 months (table S3). We then performed seven independent experiments, where in each case the hindgut contents of three worker termites were pooled, diluted, and loaded onto a digital PCR array, screening in total ~3000 individual hindgut particles (i.e., individual cells or possibly clumps of cells positive for the SSU rRNA gene).

Identification of previously unknown uncultured bacterial hosts. Of the 41 retrieved colocalizations, 28 were associated with just four phylotypes designated phage hosts I, II, III, and IV (compare Fig. 2, Table 1, and the phylogenetic analysis in fig. S4 and tables S4 and S5). Statistically, the reproducible coamplifications were significant and cannot be explained by random colocalization of two unassociated genes (Table 1). Furthermore, these associations were independently reproduced in specimens from different colonies collected 6 months apart (Fig. 2), indicative that relations between specific host bacteria and viral markers were being revealed.

All four of the phylotypes were members of the spirochetal genus *Treponema* and exhibited substantial diversity within this genus (table S4). No reproducible or statistically robust associations involving other bacteria were observed. The terminase alleles that associated with these cells shared ≥69.8% identity (average 81.9 ± 8.3% standard deviation, SD) (*33*) and were divergent

Table 1. Statistics of repeatedly colocalized SSU rRNA genes. The number of repeated colocalizations and occurrences in the reference library are based on a DOTUR analysis (tables S4 and S5). Reference library frequencies are roughly one-third of the colocalization frequencies, indicating that sampling was unbiased. The statistical test to determine the *P* value is explained in (*19*).

Host	No. of repeated colocalizations (n = 41)	Occurrence in reference library (n = 118)	*P* value (one-tailed, n = 41)
Host I	13	5	5.4×10^{-18}
Host II	8	2	7.6×10^{-13}
Host III	4	1	5.7×10^{-7}
Host IV	3	1	3.8×10^{-5}

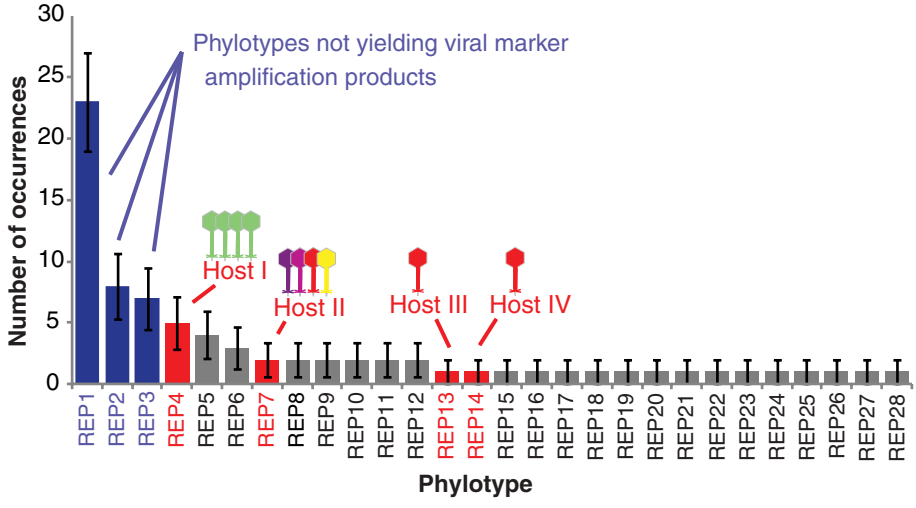

Fig. 3. Rank abundance curve of free-living *Treponema* spirochetes in *R. hesperus* termites identifying putative phage hosts. A library of 118 random chambers positive for the rRNA gene were retrieved, postamplified, and sequenced. Of these, n = 78 were related to the *Treponema* genus, corresponding to 28 different phylotypes based on an operational taxonomical unit, OTU, cut-off set by DOTUR (*41*) at 3.1%. We show these 28 phylotypes, designated as REPs, ordered by their abundance. Phylotype abundance is expected to reflect true relative abundances in the gut because single-cell amplification is not susceptible to primer bias or rRNA copy number bias. Phylotypes identified as phage hosts are marked by red bars (with the highly clonal marker associated with host I depicted by green viruses and the divergent marker associated with host II depicted by colored viruses). The most abundant free-living *Treponema* in the gut—REPs 1, 2, and 3 (blue bars)—were not associated with the viral marker. Remaining bars are gray. Error bars are estimated by the binomial SD. See table S5 for OTU assignment. Note that the isolated spirochetes were not spanned by these REPs (fig. S4).

from other currently known terminases (fig. S2), suggesting that the primer set amplifies elements exclusively found associated with termite gut treponemes. Analysis of the retrieved terminase gene sequences revealed that they are under substantial negative selection pressure with $\omega = \beta/\alpha = 0.079$, where ω is the relative rate of nonsynonymous, β, and synonymous, α, substitutions (*18*) (see table S6 for additional estimates for individual hosts). Furthermore, none of the terminase sequences in Fig. 2 appeared to encode either errant stop codons or obvious frame shift mutations, and functional motifs appeared to be conserved (fig. S2). Together, the sequence data suggest that these genes have been active in recent evolutionary history and are not degenerating pseudogenes (*19*).

Because the viral marker gene was present in hosts spanning a swath of species of termite gut treponemes, we were interested to see whether this viral marker exhibited any selectivity within this genus. The relative frequency of free-living *Treponema* phylotypes was determined by randomly sampling chambers positive for the rRNA gene (*18*) (Fig. 3 and fig. S4). We found that hosts I through IV were relatively infrequent, comprising 1.3% to 6.4% of the sampled *Treponema* cells (Table 1) and collectively about 9.8% of the sampled bacterial cells (correcting for reagent contaminants). Interestingly, the three most abundant *Treponema* phylotypes in the survey, constituting ~30, 10, and 9% of the free-swimming spirochetal cells [*Reticulitermes* environmental phylotypes (REPs) 1, 2, and 3 in Fig. 3; see also fig. S4 and table S5], were never co-retrieved with the viral marker gene to the extent that this target was spanned by our degenerate primers. Given that the degenerate core region (*17*) of each primer targets residues that were strictly conserved in gut microbes of highly divergent termite specimens (fig. S2) and that these primers successfully amplified this gene from the guts of many different termite species (see above), it appears that these strains are most likely either insensitive to this virus or that only a small percentage are infected (*19*). Therefore, we conclude that ~50% of the free-swimming spirochetal cells in the gut were likely not infected with an element encoding the targeted viral marker gene, whereas ~12% were potentially infected hosts (Fig. 3).

Phage-host cophylogeny. To elucidate the evolutionary relations between the terminase alleles and their hosts, we examined the phylogeny of the terminase genes associated with each bacterial host. Terminase alleles from *R. hesperus* formed separate clades from the clades of the two other termite species investigated in this study (clades V2 and V5 in Fig. 2). Within *R. hesperus*, different bacterial hosts exhibited different patterns of viral allelic diversity. Terminase sequences associated with host I, for example, were highly clonal, with 11 out of 13 terminase alleles sharing 96.7 ± 1.7% SD identity ($n = 11$, clade V1) (*33*). Conversely, terminase alleles associated with host II displayed marked diversity (79.1 ± 6.2% identity, $n = 11$) (*33*), deep branches, and divergent multiple alleles per bacterium for three out of eight repetitions (with 15 to 31% divergence). The unique features of the terminase alleles associated with host II compared with host I may reflect a more ancient infection or possibly an infection by a phage replicating with a lower fidelity. Alternatively, host II may be a more sensitive bacterial host susceptible to a wider range of phages. Overall, phage terminase alleles associated with different bacterial hosts were significantly divergent with only three exceptions (table S7).

The tandem trees in Fig. 2 reveal multiple possible relations between bacterial hosts and terminase alleles: Whereas host I was associated almost exclusively with a single terminase clade (V1), host II was associated with multiple terminase clades (primarily V3 and V4). Conversely, terminase clade V1 was associated almost exclusively with host I, whereas terminase clade V4 was associated with all bacterial hosts. Overall, the terminase tree was highly structured and displayed specific bacterial host–associated clades (e.g., clades V1 and V3, compare with fig. S5A). Applying the P Test (*34*) implemented in Fast UniFrac (*35*) to terminase alleles grouped by bacterial host indeed revealed significant differences between alleles associated with most pairs of hosts (table S8). Grouping terminase alleles by colony, however, did not reveal significant differences between alleles (table S9), indicating that sampling was not a factor in determining the observed host-associated heterogeneity in terminase alleles. The highly nonrandom distribution of host-associated terminase alleles therefore suggests that lateral gene transfer and/or host switching is limited in this system. This result, however, could also reflect the fact that the terminase gene does not appear to shuffle randomly among phages, possibly indicating a connection between DNA packaging and other characteristics of the phage (*36*). It remains to be seen whether other viral genes follow similar patterns.

The fact that there was little mixing between terminase alleles associated with host I (V1) and the more distantly related hosts II (V3 and V4) and III (V4), whereas alleles of the more closely related hosts II and III (table S4) exhibited a certain degree of mixing (V4), supports the notion that the probability of cross-species transmission or lateral gene transfer decreases with the phylogenetic distance of the hosts (*37*). The rRNA gene of hosts I through IV also exhibited patterns of microdiversity that may have physiological relevance (*38*, *39*). These patterns, however, were mirrored only by the terminase alleles of host III. Host I and II terminase alleles appeared to be indifferent to the bacterial host at the subspecies level.

Our results show that, in a marked departure from classical phage enrichment techniques, specific viral-host relations can be revealed in uncultivated cells harvested straight from the environment. We found that variants of a viral packaging gene appear to have infected bacterial hosts across an entire genus of bacteria. Furthermore, despite the substantial potential for lateral gene transfer and/or host switching in this well-mixed, small-volume system, the terminase tree was highly structured and displayed specific bacterial host–associated clades. It will be interesting to continue to monitor the host-virus interactions within this ecosystem as a function of space and time and across the termite community at large, shedding further light on host-virus coevolution in this unique ecosystem. More broadly, the method we have developed enables a highly parallel analysis of host-virus interactions in environmental samples from nearly any environment in nature.

References and Notes

1. C. A. Suttle, *Nat. Rev. Microbiol.* **5**, 801 (2007).
2. M. B. Sullivan *et al.*, *Environ. Microbiol.* **12**, 3035 (2010).
3. D. Lindell *et al.*, *Nature* **449**, 83 (2007).
4. F. E. Angly *et al.*, *PLoS Biol.* **4**, e368 (2006).
5. S. J. Williamson *et al.*, *PLoS ONE* **3**, e1456 (2008).
6. P. Hugenholtz, *Genome Biol.* **3**, reviews0003 (2002).
7. R. A. Edwards, F. Rohwer, *Nat. Rev. Microbiol.* **3**, 504 (2005).
8. E. A. Dinsdale *et al.*, *Nature* **452**, 629 (2008).
9. D. M. Kristensen, A. R. Mushegian, V. V. Dolja, E. V. Koonin, *Trends Microbiol.* **18**, 11 (2010).
10. A. F. Andersson, J. F. Banfield, *Science* **320**, 1047 (2008).
11. R. N. Zare, S. Kim, *Annu. Rev. Biomed. Eng.* **12**, 187 (2010).
12. E. A. Ottesen, J. W. Hong, S. R. Quake, J. R. Leadbetter, *Science* **314**, 1464 (2006).
13. Y. Marcy *et al.*, *Proc. Natl. Acad. Sci. U.S.A.* **104**, 11889 (2007).
14. L. Warren, D. Bryder, I. L. Weissman, S. R. Quake, *Proc. Natl. Acad. Sci. U.S.A.* **103**, 17807 (2006).
15. S. Dube, J. Qin, R. Ramakrishnan, *PLoS ONE* **3**, e2876 (2008).
16. F. Rohwer, R. Edwards, *J. Bacteriol.* **184**, 4529 (2002).
17. T. M. Rose *et al.*, *Nucleic Acids Res.* **26**, 1628 (1998).
18. Materials and methods are available as supporting material on *Science* Online.
19. Supporting text is available as supporting material on *Science* Online.
20. A. Tholen, B. Schink, A. Brune, *FEMS Microbiol. Ecol.* **24**, 137 (1997).
21. Y. Hongoh, M. Ohkuma, T. Kudo, *FEMS Microbiol. Ecol.* **44**, 231 (2003).
22. F. Warnecke *et al.*, *Nature* **450**, 560 (2007).
23. J. R. Leadbetter, T. M. Schmidt, J. R. Graber, J. A. Breznak, *Science* **283**, 686 (1999).
24. T. G. Lilburn *et al.*, *Science* **292**, 2495 (2001).
25. S. D. Moore, P. E. Prevelige Jr., *Curr. Biol.* **12**, R96 (2002).
26. V. B. Rao, M. Feiss, *Annu. Rev. Genet.* **42**, 647 (2008).
27. S. Chai *et al.*, *J. Mol. Biol.* **224**, 87 (1992).
28. K. Eppler, E. Wyckoff, J. Goates, R. Parr, S. Casjens, *Virology* **183**, 519 (1991).
29. S. Casjens, *Mol. Microbiol.* **49**, 277 (2003).
30. M. S. Mitchell, S. Matsuzaki, S. Imai, V. B. Rao, *Nucleic Acids Res.* **30**, 4009 (2002).
31. S. Sun *et al.*, *Cell* **135**, 1251 (2008).
32. K. D. Pruitt, T. Tatusova, D. R. Maglott, *Nucleic Acids Res.* **33**, D501 (2005).
33. Percent identity was measured across 235 unambiguous aligned amino acids.
34. A. P. Martin, *Appl. Environ. Microbiol.* **68**, 3673 (2002).
35. M. Hamady, C. Lozupone, R. Knight, *ISME J.* **4**, 17 (2010).
36. S. R. Casjens *et al.*, *J. Bacteriol.* **187**, 1091 (2005).
37. N. Wolfe *et al.*, *Glob. Change Hum. Health* **1**, 10 (2000).
38. L. Moore, G. Rocap, S. Chisholm, *Nature* **393**, 465 (1998).

39. J. R. Thompson *et al.*, *Appl. Environ. Microbiol.* **70**, 4103 (2004).
40. S. G. Acinas, R. Sarma-Rupavtarm, V. Klepac-Ceraj, M. F. Polz, *Appl. Environ. Microbiol.* **71**, 8966 (2005).
41. P. D. Schloss, J. Handelsman, *Appl. Environ. Microbiol.* **71**, 1501 (2005).

Acknowledgments: We wish to thank D. Baltimore, S. Casjens, D. S. Fisher, R. W. Hendrix, H. J. Lee, M. Lindén, E. G. Matson, R. Milo, V. J. Orphan, S. R. Quake, A. Z. Rosenthal, E. M. Rubin and colleagues at JGI, D. Z. Soghoian, N. D. Wolfe, D. Wu, X. Zhang, and the anonymous referees for their advice and feedback. We also wish to thank E.G.M. and A.Z.R for their assistance in collection of specimens and E.G.M. for ZAS genomic DNA. This project was supported by the NIH Director's Pioneer Award, NIH American Recovery and Reinvestment Act grant number R01 GM085286-01S, U.S. Department of Energy grant no. DE-FG02-07ER64484, and NSF grant nos. EF-0523267 and CMMI-0758343 and by the Davidow Family Research Fund. GenBank accession numbers are given in table S10.

Supporting Online Material
www.sciencemag.org/cgi/content/full/333/6038/58/DC1
Materials and Methods
SOM Text
Figs. S1 to S5
Tables S1 to S10
References

22 November 2010; accepted 16 May 2011
10.1126/science.1200758

REPORTS

Reconfigurable Knots and Links in Chiral Nematic Colloids

Uroš Tkalec,[1]*† Miha Ravnik,[2,3] Simon Čopar,[3] Slobodan Žumer,[1,3] Igor Muševič[1,3]*

Tying knots and linking microscopic loops of polymers, macromolecules, or defect lines in complex materials is a challenging task for material scientists. We demonstrate the knotting of microscopic topological defect lines in chiral nematic liquid-crystal colloids into knots and links of arbitrary complexity by using laser tweezers as a micromanipulation tool. All knots and links with up to six crossings, including the Hopf link, the Star of David, and the Borromean rings, are demonstrated, stabilizing colloidal particles into an unusual soft matter. The knots in chiral nematic colloids are classified by the quantized self-linking number, a direct measure of the geometric, or Berry's, phase. Forming arbitrary microscopic knots and links in chiral nematic colloids is a demonstration of how relevant the topology can be for the material engineering of soft matter.

Knots are fascinating topological objects and symbols of complexity that have fascinated the human mind since the dawn of our history. Although they are treated within the mathematical discipline of topology (*1*), knots and links have always played a prominent role in physical and life sciences (*2*). In supramolecular chemistry, complex links were demonstrated as interlinked molecular rings—catenanes—and interlocked molecules—rotaxanes (*3*–*5*). Knotting and the entanglement of polymer molecules were proved to be essential for the crystalization and rheological properties of polymers (*6*). Knotted structures have also been predicted in classical field theory (*7*), and it was recently demonstrated that the lines of zero intensity in interfering light beams can be knotted and linked as well (*8*, *9*). In biological systems, molecular knots and links are particularly important because the entanglement of DNA molecules plays the crucial role in vital processes of replication, transcription, and recombination (*10*, *11*). Knot-like topological defects have been observed in the chiral nematic liquid crystal (NLC) (*12*) but have remained unexplored because of the difficulty associated with control. The smallness of the length scales involved and the inherent lack of precise control and means of manipulating the knots and links are major obstacles in studying the structure, properties, and mechanisms of their formation.

We demonstrate knotted and linked microscopic loops of topological defects of arbitrary complexity in chiral nematic colloids. The loops are responsible for the stabilization of colloidal microparticle structures in a chiral NLC, thus forming an unusual colloidal soft matter (*13*–*16*). We performed knot and link manipulation by cutting, fusing, and reversibly reconnecting individual defect loops into knots and links of arbitrary complexity using the highly focused light of laser tweezers, which gives us full control over the knot and link formation.

The medium that supports our knots and links is a NLC with colloidal inclusions, and the strings used to tie knots and links are closed defect loops in the NLC. When spherical particles that promote alignment of NLC molecules normal to the surface are dispersed in the NLC, the direction of molecular alignment—the director—is forced to align normal to the curved and closed surface of each inclusion. Because the spherical surface makes it impossible for the molecules to fill the space uniformly, defects in the form of singular points—and in our case, closed defect loops—are created. Each particle is encircled by its own micro-loop, also called a Saturn's ring, in which the degree of molecular order is reduced in the ~10-nm-thick core, and the director exhibits fast spatial variations, making the rings visible under an optical microscope (*16*). The Saturn's ring behaves as an elastic strip that can be stretched and deformed with laser tweezers (*17*–*20*). More importantly, several Saturn's rings can be fused together by using the laser tweezers to entangle a pair or multiple colloidal particles (*21*, *22*). Here, the particles and defect loops are topologically and energetically interlinked because the loops must compensate for the topological charge of the particles (*16*) and tend to be as short as possible in order to reduce the total free energy. Although in nematic colloids with a generally homogeneous director alignment only linear entangled objects were successfully created (*22*), the defect loops in chiral NLC colloids can be optically knotted into knots and links of arbitrary complexity.

A dispersion of 4.72-μm-diameter silica microspheres in a pentylcyanobiphenyl (5CB) NLC is used in all of the experiments. The surface of the microspheres is chemically functionalized to induce a strong perpendicular alignment of the NLC molecules. The colloidal dispersion is confined to a thin glass cell, made of glass plates, coated with transparent indium tin oxide and rubbed polyimide alignment layers, spaced by a 5.5-μm-thick mylar foil (*23*). The alignment directions at the top and bottom of the cell are set perpendicular to ensure a 90° twist of the director, thus creating either left- or right-twisted chiral liquid-crystal profiles. Using twisted director structure is essential for the stability of nematic knots and links because the cell-imposed twist energetically favors effectively longer and out-of-plane deformed defect loops (Fig. 1A), which can more easily interlink.

An individual colloidal particle in the chiral nematic cell acquires a single-defect loop shown in Fig. 1A, known as a Saturn's ring (*16*). The ring is tilted at 45° with respect to the molecular alignment at the cell walls and is clearly visible because its core scatters light. In terms of topology, a closed loop without a knot in it is an unknot (*1*, *24*). We used laser tweezers to bring together several particles and observed either spontaneous or laser-assisted fusion of their rings,

[1]Condensed Matter Physics Department, Jožef Stefan Institute, Jamova 39, 1000 Ljubljana, Slovenia. [2]Rudolf Peierls Centre for Theoretical Physics, University of Oxford, Oxford OX1 3NP, UK. [3]Faculty of Mathematics and Physics, University of Ljubljana, Jadranska 19, 1000 Ljubljana, Slovenia.

*To whom correspondence should be addressed. E-mail: uros.tkalec@ijs.si (U.T.); igor.musevic@ijs.si (I.M.)
†Present address: Max Planck Institute for Dynamics and Self-Organization, Bunsenstraße 10, 37073 Göttingen, Germany.